

BOUNDARY SHEAR STRESS OF GRANULAR FLOWS

LESLIE HSU^(*), ROLAND KAITNA^(**), WILLIAM E. DIETRICH^(***) & LEONARD S. SKLAR^(****)

^(*)Department of Earth and Planetary Sciences, University of California, Santa Cruz, CA 95064, USA

^(**)Institute of Mountain Risk Engineering, University of Natural Resources and Life Sciences (BOKU), Vienna, Austria

^(***)Department of Earth and Planetary Science University of California, Berkeley, CA 94720, USA

^(****)Department of Geosciences, San Francisco State University, San Francisco, CA 94132, USA

ABSTRACT

The shear stress exerted at the bed and walls of granular flows is an important quantity for modeling and predicting runout, bulking up, channel erosion, and entrainment. Although there are some measurements of boundary shear stress for granular flows in the field and laboratory, we lack systematic measurement of shear stress for a range of flow properties such as particle size, particle shape, and fluid content, especially with natural sediment or for long durations where the flow may evolve. We used two vertically rotating drums to study the boundary shear stress

of granular flows, a smaller drum that was 56 cm diameter and 15 cm wide, and a larger drum that was 4 m diameter and 80 cm wide. The materials we used included combinations of different sized glass marbles, sand, gravel, fine sediment, and water. We compared two ways of estimating the boundary shear stress using the force balance of the particle flow in the drum. We varied particle size, particle shape, and fluid content. Larger and more angular particles increased the total boundary shear stress, as did a decrease in fluid content. This study illustrates some of the mechanisms and particle dynamics that control the boundary shear stress in natural geological flows, which has implications for debris flow modeling and hazard mitigation.

KEY WORDS: basal shear stress, experiments, particle size

MOTIVATION FROM THE FIELD AND LABORATORY

Granular flows often scour their channels and leave smooth surfaces, grooves, and scratches on the channel bed and walls (e.g. STOCK *et alii*, 2005; HSU, 2010). The polished surfaces and wear marks indicate sliding motion at the base of the flow. This contact between the flow and bed has implications for entrainment and erosion of the bed (e.g. ITOH *et alii*, 2003; STOCK & DIETRICH 2006), for modeling runout distance or mobility of the flow (e.g. MANGENEY *et alii*, 2007), and energy dissipation in the flow (e.g. BARTELT *et alii* 2006). Although we have a growing catalog of basal shear stress measurements in field and laboratory debris flows (e.g. MCARDELL *et alii*, 2007; KAITNA & RICKENMANN, 2007a, 2007b), we do not yet have a complete understanding of the flow properties and mechanisms that control local and average boundary shear stress. Properties such as particle size, particle shape, and fluid content may affect the internal velocity field and interaction with the boundary, and these properties also vary greatly throughout and between flows (IVERSON, 1997; IVERSON & VALLANCE, 2001; IVERSON *et alii*, 2010;)

Understanding the relationships between boundary shear stress and particle size, particle shape, and fluid content, may explain what controls boundary erosion or runout of granular flows..

There are measurements of basal and wall shear stress for real debris flows in the field. MCARDELL *et alii*

(2007) measured shear stress at the base of a natural debris flow in the Illgraben torrent, Switzerland. They found that average normal and shear stresses varied in-phase with flow depth, with a maximum basal shear stress value of $\tau_b = 2.8$ kPa for a flow height of 1 m. Also at the Illgraben torrent, BERGER *et alii* (2010) used a buried resistance chain to measure the timing of erosion. Contrary to intuition, they found that most erosion occurred during the watery body and not at the coarse flow front where the shear stress was a factor of seven larger than the watery body. This finding illustrates that there may not be a simple relationship between basal shear stress and erosion of underlying sediment, and other factors such as the degree of sediment saturation of the flow are important. Although polished surfaces are common, grooves and scratches are not frequent along recently scoured bedrock channels (STOCK *et alii*, 2005). However, grooves do occur, indicating localized high shear stress from large boulders over small areas, and these fluctuations from the mean stress may also be a major factor in boundary erosion and energy dissipation. The field observations so far show that we still have an incomplete understanding of topics like the controls on localized shear stresses caused by individual particles and the solid-fluid interactions that affect boundary shear stress

Basal shear stresses have also been studied in simple flows in the more controlled laboratory environment. The influence of bed sediment size and flow sediment concentration on erosion rate was studied in a suite of chute flow experiments over an erodible bed (EGASHIRA *et alii*, 2001, PAPA *et alii*, 2004). Egashira developed a nondimensional effective bed shear stress (total shear stress minus yield stress), similar to a critical Shields parameter for bed load movement, which defines a critical condition for bed material entrainment. In these experiments, some of the flows are very dilute with very low solid particle concentrations compared to natural debris flows.

Chute flows are short-lived, and for a longer period of observation, vertically rotating drums are desirable because they allow observation of a quasi-stationary flow. In a small drum of 56 cm diameter and 15 cm width, HSU *et alii* (2008) traced height profiles of various granular flows to show that flows of different particle size distribution and water content have different surface slopes and flow front positions in the drum. KAITNA & RICKENMANN (2007a, 2007b) described bulk

flow behavior by relating shear resistance to flow velocity and shear rate. They used three methods to estimate shear stress in a 2.5 m vertically rotating drum: derivation of shear stress from torque measurements at the drum axis, from shear plates embedded in the flume bottom, and from geometric considerations, similar to the force balance analysis laid out by HOLMES *et alii* (1993). Average shear stress was estimated by assuming a uniform distribution of bottom shear stress and a triangular shear stress distribution on the side walls (RICKENMANN, 1990). Shear stress estimates from torque measurements and from geometry were found to be in good agreement. Due to their location in the centre of the channel, the force plates tended to overestimate total shear stress systematically. The materials used were a homogeneous transparent liquid polymer (Carbopol Ultrez), PVC grains and a viscous natural debris flow material.

ESTIMATING BOUNDARY SHEAR STRESS

Shear stress at the bed of a debris flow is often calculated from the Coulomb model, with a linear relationship between maximum shearing strength and normal stress on the failure plane (e.g. HOWARD, 1998). More complete models separate the solid and a fluid contribution to shear stress (IVERSON 1997; IVERSON *et alii*, 2010) where the solid contribution is modeled with the Coulomb model under consideration of the effective stress concept of TERZAGHI (1936)

$$\tau_s = [\sigma_{bed} - p_{bed}] \tan \Phi_{bed} (S) \quad (1)$$

where σ_{bed} is the total basal normal stress, p_{bed} is pore pressure at the bed, and Φ_{bed} is the basal friction angle (which may be a function of the Savage number, S). Then fluid shear is estimated as

$$\tau_f = \tau_y \mu (v/h) \quad (2)$$

where τ_y is related to fluid yield stress, and μ is fluid viscosity, v is depth averaged velocity, and h is flow height (IVERSON *et alii*, 2010).

In many entrainment models, there is a threshold stress below which there is no erosion, and erosion increases monotonically with total basal shear stress above the threshold. Some numerical models assume that shear stresses are proportional to the normal

stress with constant proportionality, and also assume that effective shear stress is proportional to flow depth (e.g. LE & PITMAN, 2009). However, incomplete understanding of erosion mechanisms necessitates empirical factors to describe quantitatively the erosion of material (LE & PITMAN, 2009). In McDougall & Hungr (2005) the basal shear stress is constrained by calibration using prototype events. Medina et al. (2008) implemented a dynamic approach to entrainment, where the newly incorporated material is accelerated to the mean velocity of the flow so that the quantity of additional mass depends on the availability of momentum. These models lack incorporation of rigorous mechanistic laws relating flow dynamics to entrainment or erosion.

The existing field, laboratory, and numerical studies illustrate that there are several remaining questions about the relationship between boundary shear stress and the solid particle and fluid matrix properties. For example, how do particle size and shape affect mechanisms at the base? What controls the thickness of the shear zone? How do localized interactions affect average and fluctuating boundary shear stress? Through what mechanisms do fluid content and viscosity affect the effective normal and shear stresses? Finally, what happens when the flow is not steady, uniform, and unidirectional?

Here, we begin to address these questions by observing flows where we vary particle size, particle shape, and the amount of fluid. These properties are valuable because some of them may be inferred from a post-flow deposit in the field. To investigate the questions above, we use two vertically rotating drum flumes. We analyze two proxies for shear stress based on the force balance of a granular mass in a rotating drum. We show trends in the total shear stress with particle size, shape, and fluid content, demonstrating that predictions about boundary shear stress can be made from these solid and fluid properties.

EXPERIMENTAL METHODS

The small drum is made from a section of PVC pipe with an inner diameter of 56 cm. Both sidewalls are composed of Plexiglass, bounding a 15 cm wide channel. The drum speed was 12 RPM (0.35 m/s). The flows were monosized and were composed of either dry spherical glass marbles, dry gravel, dry sand, or moist sand. The marbles had diameters of 5,

13.8, and 25 mm while the gravel had diameters of 4, 10, and 13mm. The total mass of the flow was held constant at 3 kg.

We compared two different methods for obtaining a metric related to the total boundary shear stress. The first method is based on the force balance between the torque from the debris mass on the wheel and the drag from the flume walls on the debris mass. This method is similar to that of HOLMES *et alii* (1993) and KAITNA & RICKENMANN (2007b), where the mass was divided into smaller elements. However we found the torque from the total mass as a point mass at the centroid of the flow to be equivalent. To obtain the position of the centroid we traced the outline of the mass from a side-view photograph (e.g. Figure 2) and used ImageJ image processing software (ABRAMOFF *et alii*, 2004). We then calculated torque using the equation

$$\text{torque} = rF\sin\theta \quad (3)$$

where r is the moment arm length, F is the force on the point mass at the centroid (mass \times acceleration due gravity), and θ is the angle between the vectors for r and F . For a steady-state flow, this torque is balanced by (and therefore correlated with) the sum of shearing forces from boundary drag on the flow.

The second metric related to total boundary shear stress was the force on the chain driving the drum rotation. Figure 1 shows the set up of the system, where a force transducer (Interface Force SML- 50) measured the chain tension while the drum was spinning. The output was logged by a laptop connected to an Interface Force 9820 Digital Indicator at 4 Hz for sev-

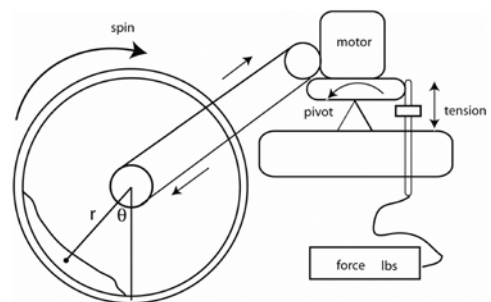


Fig. 1 - Set up of the small 56 diameter vertically rotating drum

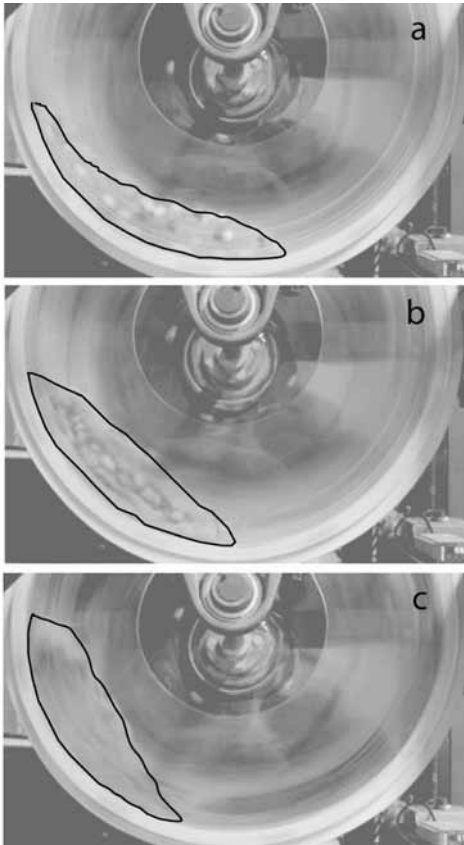


Fig. 2 - Outlines of the granular mass in the small drum at a velocity of 12 RPM. (a) Experiment S02 – glass marbles, 13.8 mm diameter; (b) experiment S06 – dry gravel, 13 mm diameter; (c) experiment S08 – moist sand, 1 mm diameter

eral rotations and the average value was used. This value, which measures the force necessary to drive the drum at a given velocity, varied for flows of the same mass but different particle compositions.

The large drum measured 4-meters in diameter and 80-cm in width. The drum was driven by a 20-kilowatt induction motor and controlled by a variable speed inverter drive. 32-mm thick Plexiglass windows allowed a side view of the flow. A 6-mm thick rubber liner with channel-spanning 25-mm tall by 25-mm wide treads, spaced every 20 cm in the stream-wise direction, prevented bulk sliding of the entire mass on the flume bed. The drum velocity for these experiments was held constant at 1.25 m/sec.

The experimental flows had between ~450 and 1200 kilograms of material, which created a shallow flow with maximum height of ~25 cm. Both mono-sized gravel-water flows and muddy flows with a wide

Exp	material	diameter mm	centroid degrees	torque N-m	reading lbs
S01	glass marbles	5	13.5	1.7	4.4
S02	glass marbles	13.8	20.8	2.6	6.3
S03	glass marbles	25	18.5	2.3	8.1
S04	gravel	4	29.5	3.6	11.5
S05	gravel	10	28.3	3.4	11.7
S06	gravel	13	32.0	3.8	11.9
S07	sand	1	31.6	3.8	11.4
S08	moist sand	1	44.2	5.0	16.7

Tab. 1. Experiments in the small 56 cm diameter

Exp	material	diameter mm	centroid degrees	torque N-m
L01	gravel and water	4	25	4116
L02	gravel and water	10	25	4260
L03	gravel and water	13	26	4379
L04	gravel and water	21	30	5074

Tab. 2 - Experiments in the large 4 m diameter drum

grain size distribution were evaluated. We tested watersaturated single-size gravel flows with mean diameters of 4, 10, 13, and 21 mm (Table 2). The 21 mm gravel were from a different source than the 4, 10, and 13 mm diameter river gravel, and were more angular in shape. In the gravel-water flows, water was added until it filled the pores, but did not run out in front of the gravel mass (HSU, 2010). Runs with a wide grain size distribution of clay, silt, sand, gravel, and cobbles were also performed (HSU, 2010). Bulk density was measured by sample tests immediately after experiments. The density was calculated with the mass of a sample of known volume of 270 cm³ and included clasts up to ~20 mm in diameter. The bulk density range was 1.9 – 2.3 g/cm³ for the muddy mixed flows and 1.9 g/cm³ for the water-saturated gravel flows.

As in the small drum experiments, we calculated a torque related to the total boundary shear stress using the position of the centroid of the mass, since the smaller drum experiments supported that this was linearly related to a direct torque measurement. The outline of the debris mass was obtained from the laser profiler. The height profile of the flow during the experiment was measured by an Acuity AR4000 laser scanner, which swept a laser line across the centerline of the flow with a rotating mirror. The laser was con-

nected to a free-standing mount and slid into place in the flume. Profiles were collected at 5 Hz. The centroid was calculated for single profiles and for the average over the experimental run. The muddy natural grain size distributions were not analyzed in the same way due to changes in total volume and water content during the flow. These experiments are described qualitatively in the results section.

The coordinate system for longitudinal position of the centroid is the drum angle, which is 0 degrees at the 6 o'clock position and increases to 90 degrees at the 9 o'clock position (mirroring the tangent to the circle for that position). In the large drum, at high drum angle (~8 o'clock position) the laser profile is ambiguous because there, the flow is thin and may be falling vertically from the drum wall instead of being a coherent part of the flow. Therefore we evaluate the outline of the flow up to the drum angle of 60 degrees, which is the transition to the detached part of the flow.

RESULTS

In the small drum, the material was placed in the drum and the motor was started at the target velocity. The mass quickly reached a near steady state position in the drum. The particle trajectories were a function of drag forces from the boundary, gravitational forces, and contact forces from other particles. A velocity field resembling a conveyor belt was established with a shear zone in the center of the flow dividing downward travelling particles at the surface and upstream travelling particles at the wall, as described in Hsu *et alii* (2008). The maximum thickness of the flow was ~5-7 cm. The shape of the particles affected the particle movement and trajectories. Perfectly spherical particles had a large component of rolling, which decreased the amount of jostling or velocity fluctuations away from the mean velocity. Subangular gravel particles had less rolling motion and more sliding and collisional or glancing interactions with their neighbors. The addition of a small amount of water to the sand flows induced cohesion between sand grains and greatly decreased internal shearing. Figure 2 shows the outline of representative flows in the small drum.

The two methods for calculating bulk shear stress correlated with each other linearly (Fig. 3). For both methods, the lowest shear stress was measured for the spherical marbles, followed by subangular gravel and sand, and finally moist sand. Within these groups,

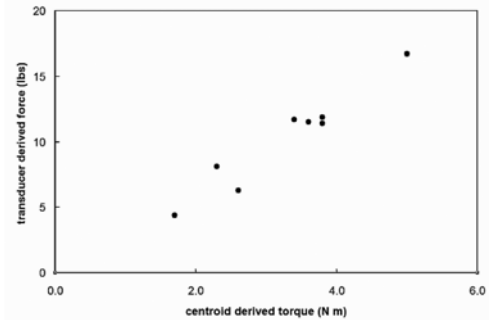


Fig. 3 - Linear trend between the centroid-derived torque on the small drum and the force transducer value, showing the correlation between the calculated and measured proxies for bulk shear stress

particle size plays a role, but it appears that particle shape and moisture/cohesion are a larger influence on boundary shear stress for the range of variables that we tested in the smaller drum. This can be seen in Table 1 as the natural sediment particles (all sizes of gravel and sand) have similar values of the shear stress metrics.

In the large drum, as the flume was started and reached the target velocity, the mass quickly found a near steady state position. There was some surging of the front due to a non-constant bed roughness. Smooth areas in the drum bed existed because the experiments had a dual purpose to measure bedrock erosion, and in each quadrant there was a 60 cm length of bed without treads where the flow passed over an erodible sample or a load plate (Hsu *et alii*, 2007). The same general particle trajectory pattern of conveyor-belt motion was established, as observed in the small drum. There was a component of lateral (cross-stream) velocity in the surface trajectories of the particles for many runs. The muddy mixtures with wide grain size distribution had a different particle trajectory velocity fields from the homogeneous gravel flows, because the different sized grains were affected by particle and wall interactions to different extent. During the ~30 minute experiment, there was some temporal variation in the bulk properties of the flow, e.g. evaporation of fluids, loss of some fines to the side walls, and bubble/foam development in the fluid. For the water-saturated gravel flows, a decrease in the centroid position was seen as time progressed. This could be either due to particle comminution and rounding, or changes in the fluid because of the bubble/foam development.

Tables 1 and 2 list the average position (in drum

angle degrees) of the centroid of the flows for different experiments. For both the marbles and gravel flows the position of the centroid is weakly correlated with gravel size, showing either a slight or unclear increasing trend with size. Particle shape has a more clear effect as all spherical marble flows have lower centroid positions than sub angular gravel or sand flows. In the large drum, increasing the particle size has a small to negligible effect on bulk shear stress (~1 degree change in the centroid for factor of three increase in gravel diameter), a larger increase in centroid position is seen for a change to a more angular 21 mm diameter gravel (4 degrees). Also, the position of the centroid is lower for water-saturated gravel in the large drum than for the same sized dry gravel flows in the small drum by 3-6 degrees, despite the additional roughness from the treads in the large drum. Using the moment arm, r , and the total mass of gravel and water, we calculate the torque for the average profile of each run (Table 2), which increases with particle size and angularity.

The experiments in the large drum with the muddy, wide grain size distributions had large clasts that were nearly equal to the height of the flow. In these multi-size flows, we observed the trajectories and wall drag effect on different size particles (HSU, 2010). The larger clasts were affected by both the sidewall and bottom boundary drag and with interactions with each other. Clasts that were about the height of the flow almost always were touching a boundary, and therefore bore a lot of drag. The increased influence of boundary drag on the larger particles resulted in an increase in the centroid position of the entire flow. Over the ~30 minute experiment, the muddy flows lost a significant amount of their fluid due to evaporation. The decrease in the matrix fluid content led to more collisional interactions between the particles, since there was less buffering by interstitial fluid. In addition, the position of the centroid appeared to increase with the loss of fluid, although it is unclear how much of this trend is due to a decrease in mass and volume in general, a decrease in the fluid content only, or an increase in the particle collisions with the bed and walls.

DISCUSSION

Natural debris flows vary spatially and temporally along their flow path with particle size, shape, and water content. Along their path, particles in the flow may become more rounded and decrease in diameter due to comminution, and the flow may become more di-

lute due to water input or drier due to evaporation and water loss. Our experiments demonstrate how minor changes in shape or fluid content may lead to a change in shear stress at the boundaries of the debris flows

The bulk shear stress is an average of locally fluctuating stresses which are highest at particle contacts with the boundary. The number of contacts and total contact area depend on the shape and size distribution of the particles. Importantly, our observations show how particle properties and dynamics play a part in determining total bulk shear stress of the flow. This role seems to be played mostly by particle shape, which affects the amount of particle locking, rolling versus sliding, and contact area and resultant drag along the boundaries. Thus, deposit characteristics can be useful for predicting boundary shear stress even if the flow itself is not observed. The size, shape, and relative amount of matrix leads to predictions about the amount of particle locking, number and size of contacts with the wall and bed, and disturbances caused by flowheight sized particles..

Although the drum geometry is different than that in nature, in these experiments most flows occupied a similar position in the drum, so that the effect of the drum geometry should be similar. The recirculation effect may be the biggest difference from nature (i.e. flows in the drum cannot deposit), although non-depositing flows are also seen in nature. Centrifugal force is a low fraction of the gravitational force at our drum velocities (HSU *et alii*, 2008).

Our experiments tested a small subset of variables that vary in natural granular flows. Some next steps are to evaluate the effect of flow velocity, bed roughness, fluid viscosity, and pore fluid pressure on the total bulk shear stress. Also, high frequency fluctuations in shear stress should be examined for information about shear stress due to particle collisions. This will help us to better understand the mechanisms causing localized shear stress at the boundaries

Numerical experiments can provide detailed information about shear stress at a higher resolution and larger spatial coverage than physical experiments. Using distinct element models to simulate granular flows of different particle shape and size will help us to understand the role of particle interactions in determining average and total shear stresses (YOHANNES, 2008). These models are also useful for exploring the effects of lateral movement and wall drag

SUMMARY AND CONCLUSIONS

Using two vertically rotating drums, we illustrated a change in the torque that balances the total boundary shear stress with changing solid and fluid properties in granular flows. We observed how particle size, particle shape, and fluid content affected the dynamics of the flows, which in turn affect the total boundary shear stress. In the experiments we conducted, we found the particle shape to be a larger influence on total shear stress than particle size. A particle shape that deviates from spherical strongly reduces rolling motion and increases collisions and velocity fluctuations from the mean velocity, increasing boundary shear stress. The addition of fluid decreased the effective normal stress by the solid component of the flow, and decreased the

shear stress. These trends in boundary shear stress with solid and fluid properties allow one to predict trends in run out, energy dissipation, and bed entrainment or erosion by natural granular flows.

ACKNOWLEDGEMENTS

The authors would like to thank Sigurd Anderson of Engineering Laboratory Design for construction of the flume. Stuart Foster, Jim Mullin, Chris Ellis, and Terry Smith assisted with the experiments and data analysis. Marisa Palucis provided helpful comments on the manuscript. This work was supported by the STC program of the National Science Foundation via the National Center for Earth-surface Dynamics under the agreement Number EAR- 0120914..

REFERENCES

- ABRAMOFF M.D., MAGALHAES P.J. & RAM S.J. (2004) - *Image Processing with Image*. J Biophotonics International, **11**(7): 36-43.
- BARTELT P., BUSER O. & PLATZER K. (2006) - *Fluctuation-dissipation relations for granular snow avalanches*. Journal of Glaciology, **52**(179): 631-643.
- BERGER C., MCARDLELL B. W., FRITSCHI B. & SCHLUNEGGER F. (2010) - *A novel method for measuring the timing of bed erosion during debris flows and floods*. Water Resources Research, **46**, W02502.
- CARPENTER A.B. & MOORE C.H. (1989) - *Isotopic and trace element constraints on the origin and evolution of saline groundwaters from central Missouri*. Geoc. Cosmoc. Acta, **53**: 383-398.
- EGASHIRA S., HONDA N. & ITOH T. (2001) - *Experimental study on the entrainment of bed material into debris flow*. Physics and Chemistry of the Earth Part C-solar-terrestrial and Planetary Science, **26**(9): 645-650.
- HOLMES R.; HUIZINGA R.; BROWN S. & JOBSON H. (1993) - *Laboratory procedures and data reduction techniques to determine rheologic properties of mass flows*. Water-Resources Investigations Report 93-4123, Technical report, U.S. Geological Survey, Rolla, Mo.
- HOWARD A.D. (1998) - *Long profile development of bedrock channels: interaction of weathering, mass wasting, bed erosion, and sediment transport*. In TINKLER K.J. & WOHL E.E, ED., Rivers Over Rock: Fluvial Processes in Bedrock Channels: 297-319.
- HSU L. (2010) - *Bedrock erosion by granular flow*, PhD thesis, University of California, Berkeley.
- HSU L.; DIETRICH W. & SKLAR L.S. (2007) - *Normal stresses, longitudinal profiles, and bedrock surface erosion by debris flows: initial findings from a large, vertically rotating drum*. In CUI P. & CHENG C., ED., Debris-Flow Hazards Mitigation: Mechanics, Prediction, and Assessment. Proceedings of the 4th International DFHM Conference Chengdu, China, September 10-13 2007.
- HSU L., DIETRICH W. E. & SKLAR L. S. (2008) - *Experimental study of bedrock erosion by granular flows*, Journal Of Geophysical Research- Earth Surface, **113**(F2), F02001.
- ITOH, T.; MIYAMOTO, K. & EGASHIRA, S. (2003) - *Numerical simulation of debris flow over erodible bed*. In RICKENMANN & CHEN, ED., Debris-Flow Hazards and Mitigation: Mechanics, Prediction, and Assessment. Proceedings of the 3rd International DFHM Conference Davos, Switzerland, September 10-12 2003.
- IVERSON R.M. (1997) - *The physics of debris flows*. Reviews of Geophysics **35**(3): 245-296.
- IVERSON R.M., LOGAN M., LAHUSEN R. G. & BERTI M. (2010) - *The perfect debris flow? Aggregated results from 28 large-scale experiments*. Journal of Geophysical Research-earth Surface, **115**, F03005.
- IVERSON R. M. AND VALLANCE, J. W. (2001) - *New views of granular mass flows*. Geology, **29**(2): 115-118.
- KAITNA R. & RICKENMANN D. (2007a) - *Flow of different material mixtures in a rotating drum*. In CUI P. & CHENG C., ED., Debris-Flow Hazards Mitigation: Mechanics, Prediction, and Assessment. Proceedings of the 4th International DFHM Conference

Chengdu, China, September 10- 13 2007.

- KAITNA R. & RICKENMANN D. (2007b) - *A new experimental facility for laboratory debris flow investigation*. Journal Of Hydraulic Research, **45**(6): 797-810.
- LE L. & PITMAN E.B. (2009) - *A Model For Granular Flows Over An Erodible Surface*, Siam Journal On Applied Mathematics **70**(5): 1407-1427.
- MANGENEY A., TSMIRING L.S., VOLFSO D., ARANSON I.S. & BOUCHUT F. (2007) - *Avalanche mobility induced by the presence of an erodible bed and associated entrainment*. Geophysical Research Letters, **34**(22), L22401.
- MCARDELL B. W., BARTELT P. & KOWALSKI J. (2007) - *Field observations of basal forces and fluid pore pressure in a debris flow*. Geophysical Research Letters, **34**(7), L07406.
- MCDougall S. & HUNGR O. (2005) - *Dynamic modelling of entrainment in rapid landslides*. Canadian Geotechnical Journal **42**(5): 1437-1448.
- MEDINA V., HURLIMANN M. & BATEMAN A. (2008) - *Application of FLATModel, a 2D finite volume code, to debris flows in the northeastern part of the Iberian Peninsula*. Landslides **5**(1): 127-142.
- PAPA M., EGASHIRA S. & ITOH T. (2004) - *Critical conditions of bed sediment entrainment due to debris flow*. Natural Hazards and Earth System Sciences, **4**(3): 469-474.
- RICKENMANN D. (1990) - *Bedload transport capacity of slurry flows at steep slopes*, PhD thesis, ETH Zurich.
- STOCK J.D. & DIETRICH W.E. (2006) - *Erosion of steepland valleys by debris flows*. Geological Society Of America Bulletin **118**(9-10): 1125-1148.
- STOCK J.D., MONTGOMERY D.R., COLLINS B.D., DIETRICH W.E. & SKLAR L. (2005) - *Field measurements of incision rates following bedrock exposure: Implications for process controls on the long profiles of valleys cut by rivers and debris flows*, Geological Society of America Bulletin, **117**(1-2): 174-194.
- TERZAGHI K. (1936) - *The shearing resistance of saturated soils and the angle between the planes of shear*. Proceedings 1st International Conference on Soil Mechanics and Foundation Engineering: 54-56.
- YOHANNES B., HILL K. M., HSU L. & DIETRICH W. E. (2008) - *Distinct Element Modeling and Large Scale Experimental Studies on Bed Stresses due to Debris Flow*. Eos Trans. AGU **89**(53), Fall Meet. Suppl., Abstract H42C-06. Banner J.L., Wasserburg G.J., Dobson P.F.,